Performance Evaluation of a Minimum Mean Square Error-Based Physical Sidelink Share Channel Receiver under Fading Channel

Yang Fu, Jaime Rodrigo Navarro, Jose F. Monserrat, Faiza Bouchmal, Oscar Carrasco Quilis

Abstract—Cellular Vehicle to Everything (C-V2X) is considered a promising solution for future autonomous driving. From Release 16 to Release 17, the Third Generation Partnership Project (3GPP) has introduced the definitions and services for 5G New Radio (NR) V2X. Since establishing a simulator for C-V2X communications is an essential preliminary step to achieve reliable and stable communication links, this paper proposes a complete framework of a link-level simulator based on the 3GPP specifications for the Physical Sidelink Share Channel (PSSCH) of the 5G NR Physical Layer (PHY). In this framework, several algorithms in the receiver part, i.e., sliding window in channel estimation and Minimum Mean Square Error (MMSE)-based equalization, are developed. Finally, the performance of the developed PSSCH receiver is validated through extensive simulations under different assumptions.

Keywords—C-V2X, channel estimation, link-level simulator, Sidelink, 3GPP.

I. INTRODUCTION

DUE to the severe car incidents caused by human factors and imperfect autonomous driving systems, Information and Communication Technology (ICT), more specifically, the next-generation cellular networks, play a critical role in future driving. Therefore, Vehicle to Everything (V2X) related research topics have attracted lots of attention from academia and industry for implementing Intelligent Transport Systems (ITS).

Two families of standards are involved in bringing vehicular communications to commercial usage: IEEE 802.11p and the 3rd Generation Partnership Project (3GPP). Dedicated Short Range Communications (DSRC) was introduced in the IEEE 802.11p standard [1]. On the other hand, Device-to-Device (D2D) communications were first mentioned in the 3GPP Rel-12 standard and later, in Rel-14, it was extended to build up LTE-V2X, the first cellular V2X (C-V2X) [2]. Furthermore, in Rel-16, LTE V2X was evolved to be supported under 5G New Radio (NR) as a fundamental enabler for further V2X applications [3]. Coming to Rel-17, more enhancements and advanced applications were discussed, such as resource allocation enhancements, UE relaying, sidelink positioning, and enhanced support of V2X operation for pedestrian UEs (i.e., UEs for Vulnerable Road Users) [4].

In an NR 5G system, there are two different operation choices for V2X networks: communication via the PC5

interface and the Uu interface. The PC5 interface supports sidelink (SL) in V2X communication for both NR and LTE. In contrast, downlink (DL) and uplink (UL) V2X communication are supported via the Uu interface for NR Non-Standalone (NSA) and Standalone (SA) 5G network architectures. Until Rel-16, only unicast communication was supported under V2X communication via the Uu interface [5]. In Rel-17, broadcast and multicast communication were discussed and enhanced in NR standards. This paper focuses primarily on the performance of the NR sidelink physical layer (PHY) through simulations.

Link-level simulations are essential to investigate the performance of the physical layer and its digital signal processing (DSP) related algorithms. In this article, we summarize the essentials of the NR sidelink PHY and report on the performance of the sidelink NR PHY employing different DSP algorithms at the receiver side. For this purpose, we developed a 3GPP-compliant MATLAB-based NR SL PHY simulator which includes the sidelink transmitter, receiver, and different 3GPP-based channel models. This paper evaluates the performance of the SL PHY under different configurations such as the number of layers, Modulation, and Coding Schemes (MCS) for different channel models. The results shown in this article are essential for researchers and developers to make informed decisions regarding the parameters involved when building or configuring the SL PHY.

The remainder of the paper is organized as follows: Section II presents the physical layer structure in the SL and briefly describes the framework of this simulator. Section III focuses on the design of the DSP-related receiver algorithms for decoding SL signals. Section IV provides the simulation results. Section V draws the conclusions of the article.

II. PHYSICAL LAYER STRUCTURE OF SIDELINK AND SIMULATOR FRAMEWORK

A. Sidelink Physical Layer Structures

There are two different protocol stacks in 5G NR systems: The user and control planes. This simulator design is focused on the user plane side. Fig. 1 shows the protocol stack design of layer 1 and layer 2 for the user plane. From Fig. 1, it can be observed that the PHY is mainly responsible for defining radio frames transmission between gNodeB (gNB) and user equipment (UE) [6].

In NR V2X SL, the physical layer architecture is designed

Yang Fu is with Polytechnic University of Valencia, Spain (e-mail: yang.fu@casa-systems.com).

World Academy of Science, Engineering and Technology
International Journal of Information and Communication Engineering
Vol:18, No:1, 2024

according to the Rel-15 NR Uu outline. Furthermore, some definitions in LTE V2X are reused in NR V2X SL physical layer processing. In the following paragraphs, a brief introduction to this structure is provided.
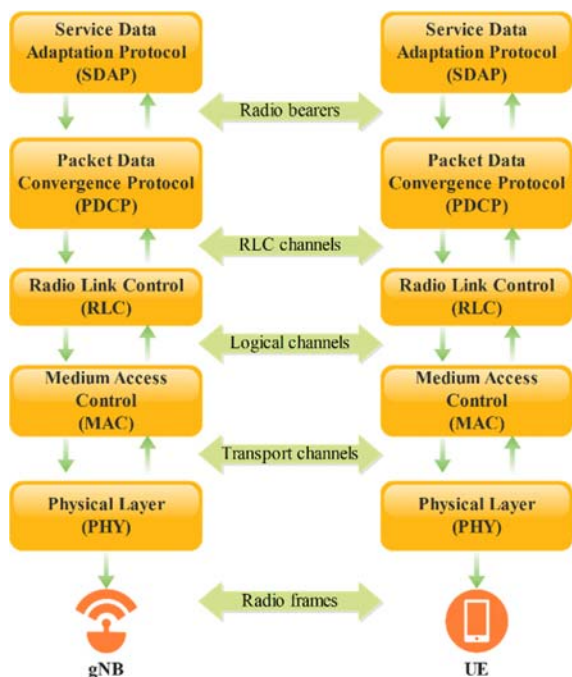

Fig. 1 User plane 5G NR protocol stack

1. *Numerology:* Theoretically, NR V2X SL should use the same frequencies as those designed for NR Uu UL and DL communications [5], which are: frequency range 1 (FR1) and frequency range 2 (FR2). For FR1, the corresponding frequency range is 410 MHz - 7.125 GHz. As for FR2, it is divided into two parts: FR2-1 (24.25 GHz - 52.6 GHz) and FR2-2 (52.6 GHz and 71 GHz).

TABLE I
SUPPORTED NUMEROLOGIES FOR NR SL

μ	SCS	Frequency Range	Cyclic Prefix	Symbols per slot	Number of slots per subframe
0	15 kHz	FR1	Normal	14	1
1	30 kHz	FR1	Normal	14	2
2	60 kHz	FR1, FR2	Normal	14	4
			Extended	12	
3	120 kHz	FR2	Normal	14	8

2. *Bandwidth part in SL*: A bandwidth part (BWP) in NR Uu is defined as a contiguous portion of bandwidth within the carrier bandwidth where a single numerology is used [7]. This definition is also employed in SL. In each carrier, only one BWP of the SL is used for all the terminals. Both transmission and receptions for SL are included within the BWP and exploit the same numerology, which means that all physical channels, including reference signals and synchronization signals, are sent within a BWP.

3. *Resource pool:* A resource pool will be composed of contiguous physical resource blocks (PRBs) and contiguous or non-contiguous slots predefined for SL communication within the BWP. In the frequency domain, the resource pool will be composed of a predefined number of contiguous subchannels "L", whose size should be 10, 12, 15, 20, 25, 50, 75, or 100 PRBs. The smallest unit for SL transmitting and receiving is a subchannel. As for the time domain, the slots for the resource pool are predefined by a bitmap. Multiple UEs can use multiple pools for SL communication, while a UE could be configured with several resource pools for receiving [8].
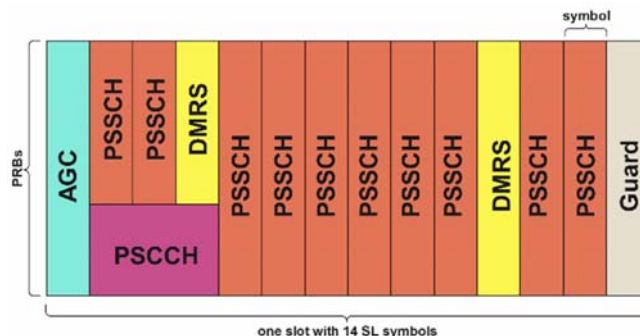

Fig. 2 Example of slot format for SL

4. *Physical channels and signals in NR V2X SL*: There are four different physical layer channels defined in NR V2X SL: Physical Sidelink Broadcast Channel (PSBCH), Physical Sidelink Control Channel (PSCCH), Physical Sidelink Shared Channel (PSSCH), and Physical Sidelink Feedback Channel (PSFCH). In addition, there are different kinds of signals transmitted on these physical channels, which are: Demodulation Reference Signal (DMRS), Sidelink Primary Synchronization Signal (S-PSS), Sidelink Secondary Synchronization Signal (S-SSS), Sidelink Channel State Information Reference Signal (CSI-RS), and Sidelink Phase Tracking Reference Signal (PT-RS) [7].

5. *Slot format of SL*: The slot format of the resource pool configured for SL comprises these different physical layer channels and reference signals. The time domain can be configured with 12 or 14 OFDM symbols with an extended or normal CP, respectively. The number of consecutive symbols assigned for SL can be set between 7 to 14 symbols, constrained by the starting symbol and number of symbols of SL. Based on subcarrier spacing and bandwidth configuration in the frequency domain, various numbers of RBs are configured for SL BWP. It is worth mentioning the number of PRBs and higher layer configurations in the SL resource pool limits the actual number of RBs used for SL. Fig. 2 shows an example of the slot configuration of SL with 12 PSSCH symbols, 2 PSSCH DMRS symbols, and 3 PSCCH symbols [7].

The SL standard defines two different types of sidelink control information (SCI), 1st stage SCI (SCI1) and 2nd stage SCI (SCI2). SCI1 is carried on PSCCH, whereas SCI2 is carried on PSSCH and multiplexed with data on PSSCH [9]. Our simulator implements the PSSCH channel as this channel also

World Academy of Science, Engineering and Technology
International Journal of Information and Communication Engineering
Vol:18, No:1, 2024

carries SCI2 data and makes it more interesting for research. In the following, we provide an overview of the PSSCH DMRS generation and the PSSCH time/frequency resource allocation [7].

The DMRS generation is similar to the Physical Uplink Shared Channel (PUSCH) in NR UL. The SL PSSCH DMRS is generated based on a pseudo-random binary sequence. First, the $r_l(m)$ sequence is generated as:

$$\frac{1}{\sqrt{2}}\big(1 - 2c(2m)\big) + j\frac{1}{\sqrt{2}}\big(1 - 2c(2m + 1)\big) \quad (1)$$

where the pseudo-random sequence c(m) is defined by:

$$c(n) = \big(x_1(n + N_c) + x_2(n + N_c)\big)mod2 \quad (2)$$

$$x_1(n + 31) = \big(x_1(n + 3) + x_1(n)\big)mod2 \quad (3)$$

$$x_2(n + 31) = \big(x_2(n + 3) + x_2(n + 2) + x_2(n + 1) + x_2(n)\big)mod2 \quad (4)$$

$N_c = 1600$ and the sequence is initialized with c_{init} as:

$$c_{init} = \big(2^{17}\big(N_{symb}^{slot}n_{s,f}^{\mu} + l + 1\big)(2N_{ID} + 1) + 2N_{ID}\big)mod\ 2^{31} \quad (5)$$

where l is the number of OFDM symbol within this slot, $n_{s,f}^{\mu}$ is the index number of this slot within this frame, $N_{ID} = N_{ID}^X\ mod\ 2^{16}$, and N_{ID}^X is the decimal value of CRC on PSCCH associated with PSSCH according to standard 38.212 [9].

After the sequence is generated, it should be mapped to an intermediate quantity based on:

$$\tilde{a}_{k,l}^{(\tilde{p}_j,\mu)} = w_f(k')w_t(l')r(2n + k') \quad (6)$$

whereas,

$$k = \begin{cases} 4n + 2k' + \Delta & \text{Configuration type 1} \\ 6n + k' + \Delta & \text{Configuration type 2} \end{cases}$$
$$k' = 0,1$$
$$l = \bar{l} + l'$$
$$n = 0,1,\dots$$
$$j = 0,1,\dots v - 1$$

Based on configuration type 1 and without transform precoding. $w_f(k')$, $w_t(l')$ and Δ are given in Table II.

TABLE II
$w_f(k')$ AND $w_t(l')$ PARAMETERS FOR PSSCH DMRS

| p | CDM group λ | Δ | $w_f(k')$ | | $w_t(l')$ |
			$k' = 0$	$k' = 1$	$l' = 0$
1000	0	0	+1	+1	+1
1001	0	0	+1	-1	+1

Finally, the intermediate quantity is multiplied by an amplitude scaling factor "Beta" configured by higher layers and mapped to the physical resources. Fig. 3 illustrates an example of the PSSCH DMRS mapping pattern based on configuration type 1.

As for resource allocation of PSSCH: in sidelink, the transmission of PSSCH is achieved with up to two antenna ports, and the antenna ports assigned to PSSCH are 1000 and 1001. First, PSSCH should transmit with associated PSCCH in the same slot, while PSSCH should be transmitted in consecutive symbols configured for sidelink. Higher layer parameters define both the start symbol and the number of symbols. It is important to notice that the PSSCH cannot be transmitted on the symbols configured with PSFCH and the last symbol assigned for sidelink. In the frequency domain, the configuration of the sub-channel position is defined by the related field in the corresponding SCI on PSCCH. The lowest sub-channel is the sub-channel transmitted on the lowest PRB of the corresponding PSSCH. If the resource of PSSCH is overlapped with PSCCH or DMRS of PSCCH, these REs could not be used for PSSCH [8].
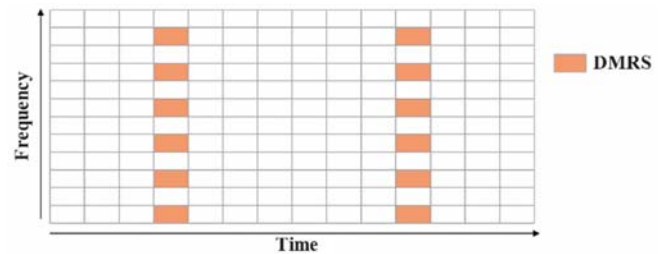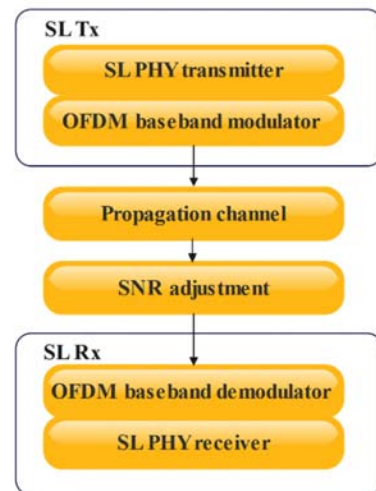

Fig. 3 An example of DMRS pattern

Fig. 4 Simulation framework

B. Simulation Framework

This section briefly introduces the simulation framework used throughout the rest of the paper. Fig. 4 shows the block diagram of the simulation framework. The simulation framework is built in MATLAB, and it consists of a PSSCH transmitter, receiver, and a channel model. Both the PSSCH transmitter and receiver closely follow the 3GPP standards and are explained in greater details in the following sections. TDLA, TDLB and TDLC channel models are supported and generated according to the guidelines provided by the 3GPP [10]. First, the PSSCH transmitter is configured with a set of

World Academy of Science, Engineering and Technology
International Journal of Information and Communication Engineering
Vol:18, No:1, 2024

parameters specific PSSCH and SCI2 which define the simulation. Then, the transmitter generates an OFDM baseband time domain signal corresponding to one slot of data and goes through one of the three supported channel models. Before entering the receiver, AWGN noise is added to the signal in order to adjust the Signal to Noise Ratio (SNR) required for the simulation. The signal is then fed into the PSSCH PHY receiver where it is OFDM demodulated and undergoes different DSP algorithms for recovering the transmitted data as explained in Section III in greater detail. The number of correct PSSCH CRCs is then counted for the slot and stored. The process is repeated for a configurable number of slots and the final BLER can be obtained by dividing the total number of correctly received PSSCH CRCs by the total number of codewords generated in all the slots of the simulation. The specific total number of codewords used for the simulations shown in this paper along with the PSSCH-related parameters are explained in greater detail in Section IV. Fig. 4 illustrates a simple framework on how the simulation was performed.

III. PHYSICAL LAYER ALGORITHM DESIGN

The 3GPP NR sidelink standard [9] defines different channel coding and rate matching for PSSCH and SCI2 both of which should be multiplexed to form one signal. The modulation scheme used for SCI2 is QPSK whereas the PSSCH modulation is configurable based on an MCS parameter which is an index to a row of a MCS Table 5.1.3.1-1 in [8] and specifies the modulation and the coding rate to be used if no additional MCS table is configured. The modulations available for PSSCH range from QPSK up to 64QAM. Thus, SCI2 and data on PSSCH need to be modulated and demodulated separately.

The PHY procedures for building a 5G NR SL transmitter are defined in the 3GPP standard [7]-[9], [11]. In the following section, we briefly describe the required steps in the transmitter with a block diagram and mainly focus on the less standardized algorithms of the receiver part.

A. Transmitter Design Workflow

For illustration, the main blocks composing a 5G PSSCH transmitter according to 3GPP [7], [9] are depicted in Fig. 5. First, SCI2 and PSSCH data bits are generated separately. Both streams of data undergo Polar and LDPC encoding for SCI and PSSCH respectively followed by individual rate matching. Then, the resulting bit-sequences need to be multiplexed together and sent for scrambling, modulation, and layer mapping. An identity matrix is used for precoding before mapping to the resource element grid. Once the resource element mapping is finished, it is used for generating OFDM symbols followed by CP addition. Finally, this time domain signal will be sent through the transmitter.

B. Receiver Design Workflow

At the receiver, the received time domain signal is firstly divided into blocks of OFDM symbols, including the CP. The CP is then removed from every OFDM symbol. Then, OFDM demodulation is performed for every symbol by means of a 4K FFT. The time-frequency resource element (RE) grid is then recovered. Depending on each simulation configuration, the PSSCH data are extracted from the subcarriers carrying PSSCH information of each OFDM symbol for further processing. Fig. 6 illustrates the block diagram of the SL receiver. In the following, a brief description of each block is provided.
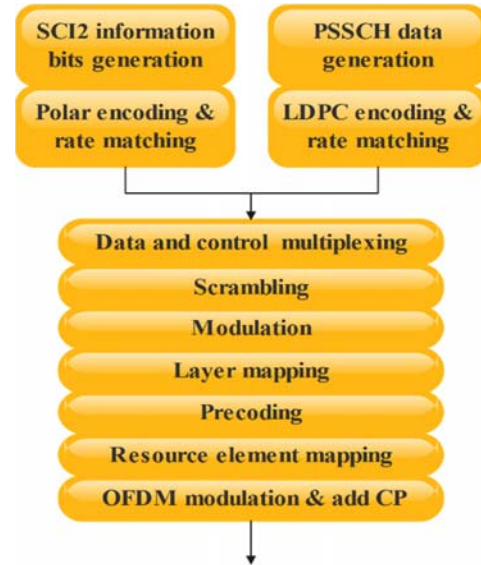

Fig. 5 Transmitter design workflow

1. Channel and Noise Estimation

The channel estimation method employed in this article is achieved through the DMRS. The SL receiver has a priori knowledge of the transmitted DMRS signal and can use it to infer the disturbance introduced by the channel at each DMRS subcarrier. In the context of MIMO and spatial multiplexing, where multiple antenna ports are used both in the transmitter and receiver, each individual channel for each transmitting and receiving antenna pair needs to be estimated. Hence, the transmitted DMRS from different antenna ports need to be separable at the receiver side. This can be achieved when all transmit DMRS antenna ports use different subcarrier indices for DMRS transmission. If two different DMRS antenna ports are configured to transmit using the same subcarrier indices, an orthogonal cover code (OCC) is used to maintain the orthogonality of the DMRS signals from the different DMRS ports. In this case, orthogonality is achieved by means of code division multiplexing (CDM). DMRS antenna ports belonging to the same CDM group employ CDM as seen in Table II.

To illustrate the channel estimation process, we consider the following transmission system model:

$$R(l,m) = H(l,m) \cdot D(l,m) + N(l,m) \qquad (6)$$

where $R(l,m)$ represents the received signal having $N_r \times 1$ dimensions being N_r the number of receive antennas. $D(l,m)$ is the transmitted QPSK modulated DMRS signal and has $N_t \times 1$ dimensions where N_t represents the number of DMRS transmitting ports. $H(l,m)$ represents the MIMO channel frequency response and has $N_r \times N_t$ dimensions. $N(l,m)$ represents an $N_r \times 1$ random variable modelling AWGN noise.

World Academy of Science, Engineering and Technology
International Journal of Information and Communication Engineering
Vol:18, No:1, 2024

The (l, m) indices represent the OFDM symbol and subcarrier indices respectively and, without loss of generality, may be dropped in the following for simplicity of illustration. For ease of illustration, we assume now one transmitting DMRS port and one receive antenna port. Then, the estimated channel between those antenna ports $\hat{H}(l, m)$ can be calculated as:

$$\hat{H}(l, m) = R(l, m) \cdot \overline{D}(l, m) \tag{8}$$

where the bar in $\overline{D}$ indicates complex conjugate. By plugging (7) into (8) it can be easily seen that the estimated channel is impaired with AWGN noise. In order to maintain a relaxed implementation complexity of the channel estimation process, we consider a rectangular fixed-size sliding window for mitigating the impact of the AWGN noise in the channel estimates. We denote $\hat{H}'(l, m)$ as the estimated channel response after the filter and W_{len} as the rectangular filter, then:

$$\hat{H}'(l, m) = \hat{H}(l, m) * W_{len} \tag{9}$$
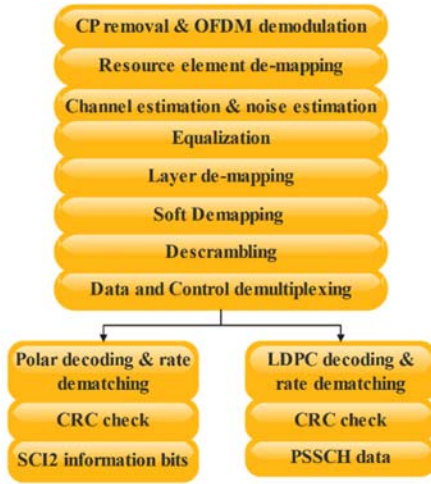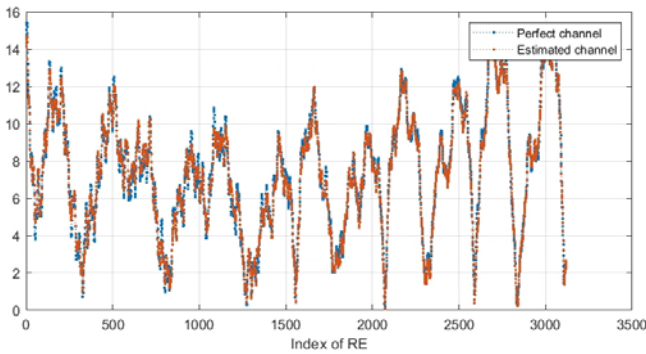

Fig. 6 Receiver design workflow

Fig. 7 Comparison between a perfect channel and an estimated channel

where * denotes convolution. The filtering is performed over consecutive DMRS subcarriers. Fig. 7 shows how the estimated channel can track the actual simulated TDLC300-100 channel model [10] for an SNR of 17dB employing a rectangular filter W_{len} of 7 taps.

Noise estimation is needed during the MMSE equalizer as explained in the next section. The noise covariance matrix can be estimated by measuring the noise rejected by the rectangular filter as:

$$\hat{N}(l, m) = R(l, m) - \hat{H}'(l, m) \cdot D(l, m) \tag{10}$$

Thus, the noise covariance matrix can be derived as:

$$\sigma^2 = E\{NN^H\} \tag{11}$$

where $E\{\cdot\}$ denotes expectation.

2. MMSE Equalizer

MMSE equalization provides a good performance versus complexity tradeoff and is the type of equalizer chosen for the SL signal equalization in this article. In the following, we derive the MMSE expression. We consider the following signal transmission model:

$$Y = H \cdot X + N \tag{12}$$

where Y represents the received signal having $N_r \times 1$ dimensions being N_r the number of receive antennas. X is the transmitted signal and has $N_t \times 1$ dimensions where N_t represents the number of DMRS transmitting ports. H represents the MIMO channel frequency response and has $N_r \times N_t$ dimensions. N represents an $N_r \times 1$ idd random variable modeling AWGN noise. The aim of the MMSE estimator is to find a suitable G matrix to equalize the received signal Y such that the error $e = GY - X$ is minimized. Since the received signal is uncorrelated with the noise we have:

$$E\{Y \cdot e^H\} = 0 \tag{13}$$

where the subscript "H" denotes Hermitian operation. The above equation can also be written as:

$$E\{e \cdot Y^H\} = 0 \tag{14}$$

Expanding this equation, we get:

$$E\{(GY - X) \cdot Y^H\} = 0 \tag{15}$$

and:

$$G = E\{XY^H\}E\{YY^H\}^{-1} \tag{16}$$

Further expanding each term of (16) we get:

$$E\{XY^H\} = E\{(HX + N)(X^H H^H + N^H)\} = E\{HXX^H H^H + HXN^H + NX^H H^H + NN^H\} = H(PI)H^H + \sigma^2 I \tag{17}$$

where P is the power of transmitted signal and σ is noise variance. Equation (17) assumes that the noise is uncorrelated (there are no interferers) and the covariance matrix is just a diagonal matrix. Similarly, we can obtain:

World Academy of Science, Engineering and Technology
International Journal of Information and Communication Engineering
Vol:18, No:1, 2024

$$E\{YY^H\}^{-1} = (PI)H^H \qquad (18)$$

Thus, finally G can be derived as:

$$G = H^H \left(HH^H + \frac{\sigma^2}{P}I \right)^{-1} \qquad (6)$$

H and σ are already known to the receiver from the channel and noise estimation modules as explained in the previous section. The receiver can assume $P = 1$ such that the signal after equalization will be power normalized which will aid the soft-demapping module later.

Figs. 8 and 9 show the constellations before and after MMSE equalization for a 64QAM PSSCH signal having 17 dBs of SNR. From the figures, we can perceive the correct behavior of the MMSE equalization. Detailed configuration of the signals in Figs. 8 and 9 can be found in Section IV.
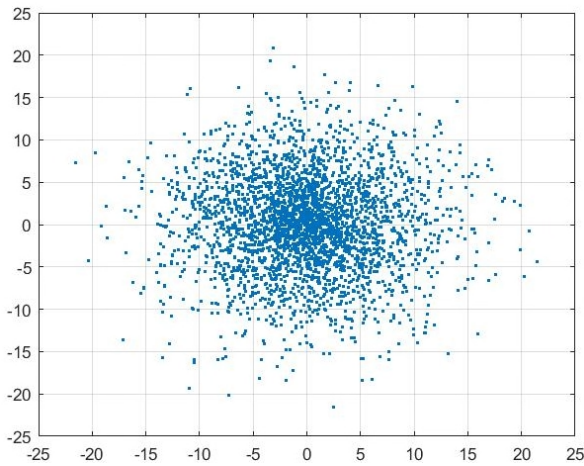

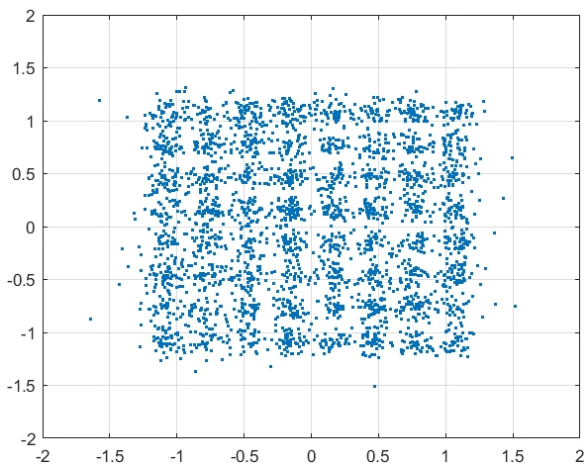Fig. 8 Constellation before the equalizer

Fig. 9 Constellation after the equalizer

3. Procedures for Restoring Data

After channel estimation, noise estimation and MMSE equalization, the resulting signal shall go through layer de-mapping, soft demodulation, and descrambling as shown in Fig. 6. As mentioned before, SCI2 and data on PSSCH are multiplexed together before scrambling in the transmitter. Therefore, demultiplexing before channel decoding is also necessary. After demultiplexing control information with data, SCI2 data are polar decoded whereas PSSCH needs to be LDPC decoded. Finally, to show the performance of our PSSCH receiver, we count the number of CRCs passed for computing the Block Error Rate (BLER).

IV. SIMULATION RESULTS AND ANALYSIS

To evaluate the functionality and performance of the developed PSSCH receiver, we conducted simulations with two types of modulation schemes under different TDL channel models defined by 3GPP standards [10]. All the details regarding the simulation parameters are shown in Table III. The performance of the proposed PSSCH receiver structure is given by means of BLER versus SNR graphs.

TABLE III
SIMULATION PARAMETERS

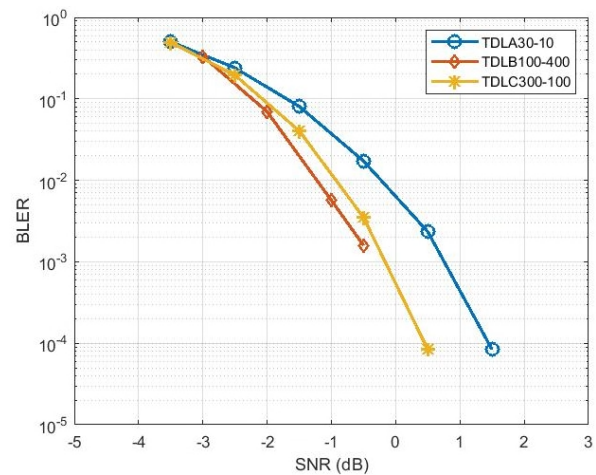| Name of simulation parameters	Configured value
Carrier frequency/GHz	3.5016
Bandwidth/MHz	100
Numerology μ	1
Subcarrier spacing/kHz	30
Number of DMRS symbols	2
Number of simulation slots	3000/500
Channel type	TDL model
Number of configured RBs	260
Number of PSSCH symbols	12
Modulation Scheme	QPSK/64QAM
Iterations of LDPC decoder	8

Fig. 10 BLER vs. SNR for different TDL model, 2T2R, MCS0, QPSK

Fig. 10 shows the BLER versus SNR performance of the proposed PSSCH receiver under QPSK modulation scheme, MCS 0 with 0.2344 spectral efficiency [8] under three different TDL channel models: TDLA30-10, TDLB100-400 and TDLC300-100. This simulation is measured under two transmit antennas (two layers) and two received antennas (2T2R). From Fig. 10 we can observe that the proposed PSSCH receiver

World Academy of Science, Engineering and Technology
International Journal of Information and Communication Engineering
Vol:18, No:1, 2024

achieves a good performance under different channel models. BLERs below 10^{-3} can be reached for all channel models for SNRs larger than 0 dB.
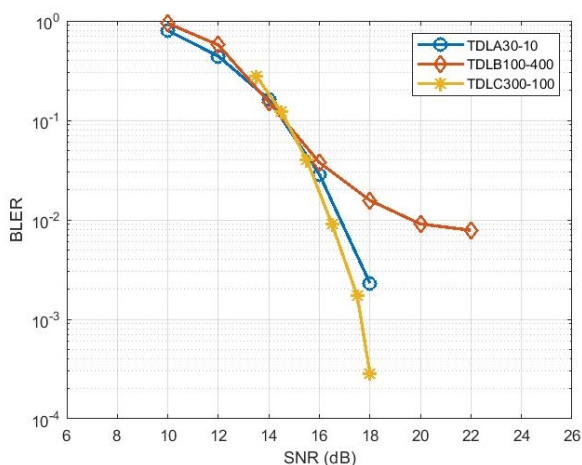

Fig. 11 BLER vs. SNR for different TDL model, 1T2R, MCS20, 64QAM

Fig. 11 shows the BLER versus SNR performance of the proposed receiver for a 64QAM PSSCH transmission with MCS 20, having 3.3223 of spectral efficiency. The antenna configuration for this case is one transmit antenna and two receive antennas (1T2R). As expected, a much higher SNR is required to achieve the same BLER compared to MCS0 in Fig. 10. It is observed that, for the TDLB100-400 case, there exists an error floor. The error floor can be explained by the 400 Hz doppler which makes the channel change faster in time and cannot be adequately tracked with only 2 DMRS symbols and current channel estimation methods. Hence, these channel estimation imperfections result in an error floor. Besides, the modulation scheme is 64QAM, and the LLR is easily wrongly decoded.

V. CONCLUSION

This paper has presented a link-level simulator based on 5G NR sidelink emphasizing PSSCH transmitter and receiver development. The transmitter of this simulator has been established based on the 3GPP specifications for the physical layer. As for the receiver part, considering the complexity of implementation, we have chosen a DMRS-based channel estimation with a rectangular shaped filter to mitigate AWGN noise for estimating the channel, whereas the MMSE algorithm was utilized for the equalization part to estimate the channel coefficient for the first trial. The functionality test under 64QAM has been shown to demonstrate that the receiver can successfully demodulate the data. Extensive simulations have also been conducted to analyze and evaluate the performance of the current simulator with different modulation schemes for several fading channels defined by 3GPP channel model specifications.

From the simulation results, we notice that there is still room for improvement. In future work, we plan to optimize the channel estimation to provide a more accurate estimation of channel coefficients for larger doppler and higher modulation schemes. We also plan to add timing and frequency offset estimation to make compensation and then retrieve more solid results.

REFERENCES

[1] D. Garcia-Roger, E. E. González, D. Martín-Sacristán and J. F. Monserrat, "V2X support in 3GPP specifications: From 4G to 5G and beyond," in IEEE Access, vol. 8, pp. 190946-190963, 2020, doi: 10.1109/ACCESS.2020.3028621.
[2] TSG SA, Release Description; Release 14, document TR 21.914 V14.0.0, 3GPP, Jun. 2018.21914.
[3] TSG SA, Release Description; Release 16, document TR 21.916 V0.4.0, 3GPP, Mar. 2020.21916.
[4] TSG SA, Release 17 Description; Summary of Rel-17 Work Items, document TR21.917 V0.5.0, 3GPP, Apr.2022.
[5] M. H. C. Garcia et al., "A Tutorial on 5G NR V2X Communications," in IEEE Communications Surveys & Tutorials, vol. 23, no. 3, pp. 1972-2026, third quarter 2021, doi: 10.1109/COMST.2021.3057017.
[6] 3GPP, TR 38.300, NR and NG-RAN Overall description; Stage-2 (V17.3.0, Release 17), 3GPP Standard, Dec. 2022.
[7] 3GPP, TS 38.211 NR; Physical Channels and Modulation (V17.1.0, Release 17), 3GPP Standard, Mar. 2022.
[8] 3GPP. TS 38.214. NR; Physical layer procedures for data (V17.1.0, Release 17), 3GPP Standard, Mar. 2022.
[9] 3GPP. TS 38.212. NR; Multiplexing and channel coding (V17.1.0, Release 17), 3GPP Standard, Mar. 2022.
[10] 3GPP. TR 38.901. Study on channel model for frequencies from 0.5 to 100 GHz (V17.0.0, Release 17), 3GPP Standard, Mar. 2022
[11] 3GPP. TS 38.213. NR; Physical layer procedures for control (V17.1.0, Release 17), 3GPP Standard, Mar. 2022